BIOCHEMISTRY
including biophysical chemistry & molecular biology

Article

pubs.acs.org/biochemistry

Structural and Mechanistic Analysis of a Novel Class of Shikimate Dehydrogenases: Evidence for a Conserved Catalytic Mechanism in the Shikimate Dehydrogenase Family

James Peek,[†] John Lee,[†] Shi Hu,[†] Guillermo Senisterra,[‡] and Dinesh Christendat*[,†,§]

[†]Department of Cell and Systems Biology, University of Toronto, Toronto, Ontario, Canada M5S 3B2

[‡]Structural Genomics Consortium, University of Toronto, Toronto, Ontario, Canada M5G 1L7

[§]Centre for the Analysis of Genome Evolution & Function, University of Toronto, Toronto, Ontario, Canada M5S 3B2

ABSTRACT: Shikimate dehydrogenase (SDH) catalyzes the reversible NADPH-dependent reduction of 3-dehydroshikimate to shikimate. This reaction represents the fourth step of the shikimate pathway, the essential route for the biosynthesis of the aromatic amino acids in plants, fungi, bacteria, and apicomplexan parasites. The absence of this pathway in animals makes it an attractive target for herbicides and antimicrobials. At least four functionally distinct enzyme classes, AroE, YdiB, SDH-like (SdhL), and AroE-like1 (Ael1), utilize shikimate as a substrate in vitro and form the SDH family. Crystal structures have been determined for AroE, YdiB, and SdhL. In this study, we have determined the first representative crystal structure of an Ael1 enzyme. We demonstrate that Ael1 shares a similar overall structure with the other members of the SDH family. This high level of structural conservation extends to the active sites of the enzymes. In particular, an ionizable active site lysine and aspartate are present in all SDH homologues. Two distinct biochemical roles have been reported for this Lys-Asp pair: as binding residues in YdiB and as a catalytic dyad in AroE and SdhL. Here, we establish that the residues function as a catalytic dyad in Ael1 and, interestingly, in at least one YdiB homologue. The conservation of three-dimensional fold, active site architecture, and catalytic mechanism among members of the SDH family will facilitate the design of drugs targeting the shikimate pathway.

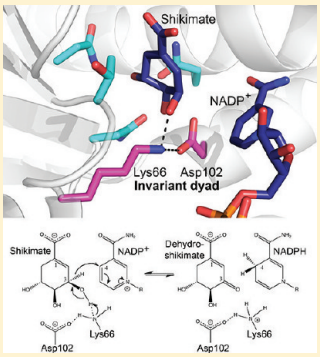

The shikimate pathway is an essential route for the biosynthesis of the aromatic amino acids, quinines, vitamins, and folates in plants, fungi, bacteria, and apicomplexan parasites.[1−3] The absence of the pathway in metazoans makes it an attractive target for herbicides and antimicrobials.[4,5] Indeed, the widely used herbicide glyphosate competitively inhibits enolpyruvylshikimate-3-phosphate (EPSP) synthase, the sixth enzyme in the pathway.[6,7] However, the emergence of glyphosate resistance in a number of weed species and the growing need for novel antibiotics effective against highly resistant pathogenic bacteria provide a strong rationale for identifying new inhibitors of the shikimate pathway.[8,9]

The fourth reaction in the shikimate pathway, the reversible NADPH-dependent reduction of dehydroshikimate to shikimate, is catalyzed by shikimate dehydrogenase (SDH), AroE.[10,11] *Escherichia coli* loss of function *aroE* mutants are incapable of growth without supplementation of the aromatic amino acids, demonstrating the physiological significance of the enzyme.[10,11] Because of its central role in the shikimate pathway, and hence in basic metabolism, AroE represents an appealing drug target.[4,5,12] However, the process of designing inhibitors of AroE could be complicated by the existence of additional SDH homologues that retain an ancestral affinity for shikimate.[13] These enzymes could compromise the efficacy of drugs acting on AroE by functionally compensating for the inhibited enzyme, a prospect that warrants a detailed assessment of their structural and mechanistic relatedness.

Three close homologues of AroE have been biochemically characterized: YdiB, SDH-like (SdhL), and AroE-like1 (Ael1).[13−15] YdiB is an NAD^+-dependent quinate/shikimate dehydrogenase implicated in quinate metabolism, a process that shares the intermediates dehydroquinate and dehydroshikimate with the shikimate pathway.[14,16,17] SdhL from *Haemophilus influenzae* catalyzes the oxidation of shikimate but with a turnover rate much lower than that of AroE;[15] a bona fide biological function for the enzyme has yet to be demonstrated. Ael1 is a recently annotated, functionally distinct SDH subclass that binds shikimate with high affinity and also exhibits measurable activity with quinate.[13] We previously proposed that the enzyme acts at a novel branchpoint of the shikimate pathway.[13] Ael1 from *Pseudomonas putida* possesses a sequence 54% identical with that of the AroE enzyme from the same organism, while it is ∼25 and ∼20% identical with those of YdiB- and SdhL-type enzymes, respectively (Figure 1).

Representative crystal structures have been determined for the AroE, YdiB, and SdhL subclasses.[14,15,18−25] The structures of these enzymes share a similar three-dimensional fold. Moreover, key active site residues are highly conserved. These residues include an invariant lysine and aspartate, which have been reported to act as a catalytic dyad in the AroE and SdhL

Received: April 17, 2011
Revised: August 15, 2011
Published: August 16, 2011

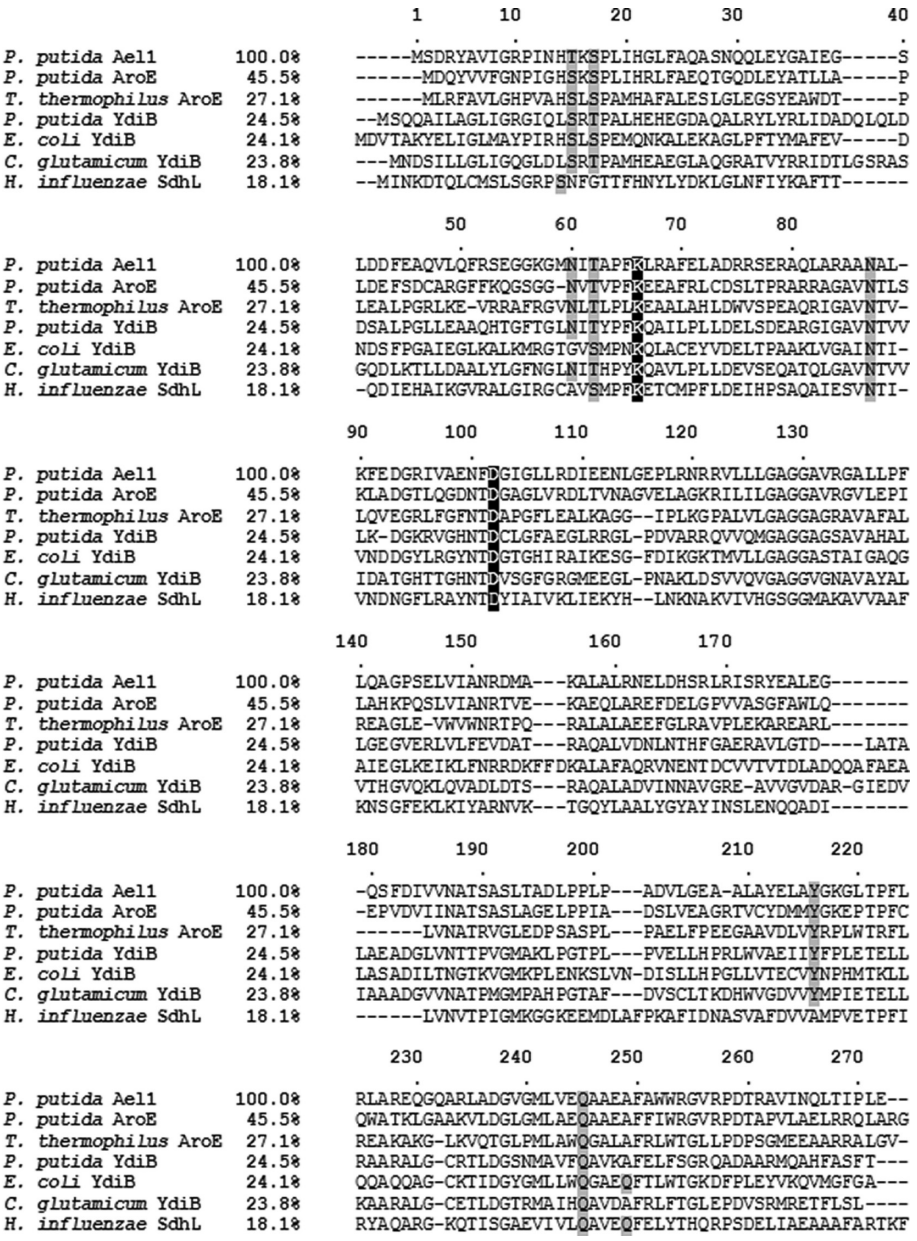

Figure 1. Sequence alignment of representative members of the SDH family demonstrating the high level of conservation of key substrate binding site residues among SDH homologues. Substrate binding residues are highlighted in gray. The strictly conserved active site lysine and aspartate are highlighted in black. Percent sequence identities of the different SDH homologues relative to Ael1 are provided for comparison.

subclasses.[15,20,24] Surprisingly, however, the residues reportedly function in substrate binding instead of catalysis in a YdiB enzyme from *E. coli*, suggesting that the YdiB subclass has evolved a distinct catalytic mechanism.[26] The apparent existence of multiple SDH mechanistic classes could complicate the design of drugs targeting the active sites of the enzymes.

In this study, we address two aspects of the SDH family: the conservation of three-dimensional structure and the conservation of catalytic mechanism among SDH homologues. We have determined the first crystal structure of an Ael1 enzyme, allowing us to perform a comprehensive structural analysis of the SDH family. We observe a high level of structural conservation between *P. putida* Ael1 and other SDH homologues in terms of both overall three-dimensional fold and active site architecture. We explore the catalytic mechanism employed by Ael1 by site-directed mutagenesis and show that, like the corresponding residues in AroE and SdhL, the conserved active site lysine and aspartate are essential for the reaction catalyzed by Ael1. Interestingly, we have also determined by mutagenesis that these residues play a key role in catalysis, but not substrate binding, in a YdiB enzyme from *P. putida*, in contrast to their reported role in the YdiB enzyme from *E. coli*.[26] Our findings therefore establish a common catalytic mechanism for the members of the SDH family, with the possible exception of only some enzymes in the YdiB subclass. Evidence of structural and mechanistic conservation in the SDH family will facilitate rational approaches to targeting the enzymes for drug design.

MATERIALS AND METHODS

Protein Expression and Purification. The genes encoding Ael1, AroE, and YdiB from *P. putida* KT2440 were

amplified via polymerase chain reaction (PCR) from genomic DNA as previously described.[13] The PCR products were cloned into a modified pET28a vector (Novagen, Gibbstown, NJ) with a six-His-tag/TEV cleavage site (provided by the Structural Genomics Consortium, University of Toronto). Recombinant proteins were expressed in *E. coli* strain BL21 CodonPlus grown in 1 L of Luria-Bertani medium with 50 μg/mL kanamycin. Cultures were incubated in a shaker at 37 °C until they reached an OD_{600} of 0.6−0.8 and then induced with 0.4 mM isopropyl β-D-thiogalactopyranosids (IPTG) for 4 h with shaking at 37 °C. Cultures were subsequently incubated overnight with shaking at 16 °C. Cells were harvested by centrifugation and lysed using a French press followed by sonication. Insoluble cellular materials were removed following centrifugation. Protein purification was performed by nickel-nitrilotriacetic acid (Ni-NTA) affinity chromatography, using buffers containing 50 mM Tris-HCl (pH 7.5), 500 mM NaCl, 5% glycerol, and increasing concentrations of imidazole (5 mM for column equilibration, 30 mM for column washes, and 300 mM for elution of proteins of interest). Following purification, the proteins were dialyzed for 4 h at 4 °C in 500 mM NaCl, 10 mM Tris-HCl (pH 7.5), and 5% glycerol. To examine the oligomeric state of Ael1 and YdiB, the purified proteins were subjected to size exclusion chromatography using an AKTA purifier system (GE Healthcare, Uppsala, Sweden) with a HiLoad 16/60 Superdex 75 column.

Site-Directed Mutagenesis. The following forward primers were used to introduce mutations into the plasmids encoding wild-type Ael1 or YdiB (substituted codons are underlined): Ael1 T15S, GACCGATCAACCACTCCAAGTCCCCGCTG; Ael1 K66N, TCACCGCCCCGTTCAACCTGCGTGCC; Ael1 F101T, GCATCGTCGCCGAAAACACCGATGGCATCGGTTTGC; Ael1 D102N, CGTCGCCGAAAACTTCAATGGCATCGGTTTGCT; YdiB K74A, CATTACCTACCCGTTCGCGCAGGCGATCCTGCCG; YdiB K74N, TGAACATTACCTACCCGTTCAACCAGGCGATCCTG; YdiB D110A, CGGCCACAACACCGCTTGCCTGGGCTTTG; YdiB D110N, GTCGGCCACAACACCAATTGCCTGGGCTTTG. Mutations were introduced by incubating the Ael1 or YdiB wild-type template plasmid with mutagenic forward and complementary reverse primers, dNTPs, and *Pfu* DNA polymerase in a PCR mixture using the protocol described in the QuikChange manual (Stratagene). Following the PCR, wild-type template plasmid was digested using DpnI and the reaction mixture was transformed into *E. coli* XL1-blue cells. Plasmid DNA was purified from the transformed bacterial cells using a plasmid miniprep kit (Sigma-Aldrich), and mutations were verified by DNA sequencing. Mutant proteins were expressed and purified as described above.

Enzyme Kinetics. The activity of wild-type and mutant enzymes was measured by monitoring the reduction of $NAD(P)^+$ (ε = 6220 M^{-1} cm^{-1}) at 340 nm in the presence of shikimate or quinate. Reactions were conducted in triplicate at 25 °C in 150 mM NaCl and 50 mM Tris-HCl (pH 8.8) in a total reaction volume of 1 mL. V_{max} and K_m values were determined by varying either the amount of substrate or the amount of cofactor while keeping the other at saturation. Two millimolars of substrate or cofactor was considered saturating for wild-type Ael1 and AroE and for Ael1 mutants; 5 mM was used for YdiB wild-type and mutant enzymes. Data analysis was performed using GraFit.[27] Data were fit to eq 1

$$v = V_{max}[S]/(K_m + [S]) \quad (1)$$

where v is the initial velocity and $[S]$ is the concentration of the varied substrate (or cofactor), to obtain maximal velocity values (V_{max}) and the Michaelis constant (K_m).

Differential Static Light Scattering Assay. Binding of substrates by YdiB wild-type and mutant enzymes was evaluated by a differential static light scattering (DSLS) experiment using the Stargazer platform (Harbinger Biotech, Toronto, ON).[28] All samples were prepared in buffer composed of 250 mM NaCl and 25 mM Tris-HCl (pH 7.5). Protein solutions (50 μL at 0.4 mg/mL) were incubated with the substrate quinate (0, 0.5, 1, 2, and 4 mM) and heated in increments of 1 °C/min from 25 to 85 °C in a clear bottom 384-well plate. Four replicates were performed for each substrate concentration. The intensities of light scattered by the samples were measured in 30 s intervals using a charge-coupled device camera, plotted as a function of temperature and fitted with the Boltzman equation by nonlinear regression. The inflection point of each aggregation curve, T_{agg} (temperature of aggregation), represents the temperature at which 50% of the protein is aggregated. ΔT_{agg} values were determined by subtracting the T_{agg} of samples without ligand from the T_{agg} of samples incubated with ligand. ΔT_{agg} values of >2 °C were found to lie outside experimental error and were considered to indicate substrate binding. For additional analysis, intensity values were converted to values representing the fraction of total protein aggregated, F_a, using eq 2

$$F_a = (I_{obs} - I_{min})/(I_{max} - I_{min}) \quad (2)$$

where I_{obs} is the measured intensity at a given temperature and I_{min} and I_{max} are the mimimum and maximum intensities, respectively, measured across all temperatures.

Protein Crystallography and Structure Determination. Protein crystals were generated by the hanging drop vapor diffusion method. Ael1 crystals were produced under a crystallization condition consisting of 0.1 M NaHEPES (pH 7.5), 2 M $(NH_4)_2SO_4$, and 1.5% PEG400. Crystals formed in drops containing 2 μL of protein (10 mg/mL stock concentration) and 2 μL of crystallization solution.

Diffraction data were collected at the Advanced Photon Source at the Argonne National Laboratory on beamline 19-ID. A summary of the data collection and refinement statistics is given in Table 1. Data were processed and scaled using HKL2000.[29] The crystal structure of Ael1 was determined at 1.7 Å resolution by molecular replacement with *H. influenzae* AroE [Protein Data Bank (PDB) entry 1P74] using AMORE,[30,31] with manual building performed using COOT[32] followed by refinement with REFMAC.[33] A final refinement was performed using PHENIX.[34] The atomic coordinates and structure factors for Ael1 were deposited as PDB entry 3PWZ.

RESULTS

Kinetic Properties of Ael1. Ael1 has a distinct biochemical profile that differentiates it from other members of the SDH family. The kinetic properties of *P. putida* Ael1 were determined by a steady state assay using the recombinant enzyme in the presence of shikimate or quinate and $NAD(P)^+$. For comparison, we have also determined the kinetic properties of *P. putida* AroE. The kinetic profiles of Ael1 and AroE are

Table 1. Summary of X-ray Crystallographic Data Collection and Refinement Statistics

Data Collection Statistics	
space group	*C*121
unit cell (Å)	103.28 × 49.45 × 60.51
α, β, γ (deg)	90.0, 114.4, 90
no. of molecules in the asymmetric unit	1
resolution (Å)	1.7
total no. of observations	52139
no. of unique reflections	27408
intensity ($I/\sigma\langle I\rangle$)	18.2 (2)
completeness (%)	90 (57)
R_{sym} (%)	0.081 (0.464)
Refinement Statistics	
resolution (Å)	1.7
R_{work}/R_{free}	21.4/24.4
σ cutoff	0.0
rmsd for bond lengths (Å)	0.007
rmsd for dihedral angles (deg)	1.07
no. of protein atoms	2085
no. of solvent molecules	148
Ramachandran plot analysis (%)	
favored regions	89.7
additional allowed regions	10.3
disallowed regions	0

shown in Table 2 and are consistent with the previously reported values for the enzymes.[13] The activity of Ael1 is strongly pH-dependent, with a catalytic basic group titrating at pH 6.8 (data not shown). The enzyme has a pH optimum of 8.5. Both Ael1 and AroE preferentially utilize $NADP^+$ instead of NAD^+. With $NADP^+$ held at saturation, we determined a K_m of 5.7 ± 0.6 μM for Ael1 with respect to shikimate. This value is 31-fold lower than the Michaelis constant of *P. putida* AroE (K_m = 178 ± 14 μM) and is among the lowest of any previously characterized member of the SDH family.[4,13−15,20,21,24,35,36] In contrast, Ael1 exhibits a 39-fold lower k_{cat} (7.9 ± 0.2 s^{-1}) than AroE (307 ± 7 s^{-1}). Ael1 is also differentiated from AroE by its ability to use quinate as a substrate. However, with quinate, it exhibits a high Michaelis constant (K_m = 3680 ± 380 μM) and low turnover rate (k_{cat} = 0.14 ± 0.01 s^{-1}) compared to those of the quinate/shikimate dehydrogenase (YdiB) from *P. putida* (Table 3). This finding implies that quinate is not the favored substrate of Ael1.

General Description of the Ael1 Crystal Structure. While crystal structures have been determined for enzymes in the AroE,[18,20−22,24] YdiB,[14,23] and SdhL[15] subclasses, no structure was previously available for an Ael1 enzyme. Here, we have determined the crystal structure of *P. putida* Ael1 to 1.7 Å resolution (Figure 2a). The Ael1 protomer is 272 amino acids in length, and its crystals belong to the *C*121 space group. A single protein molecule occupies each asymmetric unit in the Ael1 crystal lattice. In addition, analysis by size exclusion chromatography suggests that Ael1 is a monomer in solution.

Ael1 exhibits a highly conserved three-dimensional fold characteristic of proteins in the SDH family.[14,15] Its overall structure consists of two domains, both belonging to the α/β class of proteins (Figure 2a). The N-terminal domain, encompassing residues 1−100, is composed of a series of five β-strands in β2, β1, β3, β4, β5 strand order flanked by α-helices α11, α1, α2, α3, and α4. The C-terminal domain adopts a Rossmann fold, consisting of a six-stranded β-sheet in β8, β7, β6, β9, β10, β11 strand order surrounded by helices α6, α7, η1, η2, α8, and α9. The N- and C-terminal domains of the protein are connected centrally by α-helices α5 and α10, which form the back wall of a deep cleft (Figure 2b). Main chain alignments of Ael1 and representative structures of AroE from *Thermus thermophilus* (PDB entry 1WXD), YdiB from *Corynebacterium glutamicum* (PDB entry 2NLO), and SdhL from *H. influenzae* (PDB entry 1NPY) produce rmsd values of 1.762, 2.801, and 2.899 Å, respectively, demonstrating the high level of similarity in the overall structures of members of the SDH family (Figure 2c).

Cofactor Binding Site. The Ael1 cofactor and substrate binding sites are located in the deep cleft between the two

Table 2. Kinetic Properties of Ael1 and AroE Wild-Type Enzymes and Ael1 Mutant Variants[a]

enzyme	parameter	SA(nadp)	NADP(sa)	SA(nad)	NAD(sa)	QA(nadp)	NADP(qa)
Ael1 WT	k_{cat} (s^{-1})	7.9 ± 0.2	8.4 ± 0.2	35.5 ± 0.8	96.6 ± 3.5	0.14 ± 0.01	0.039 ± 0.0007
	K_m (μM)	5.7 ± 0.6	12.0 ± 1.3	630 ± 32	3286 ± 197	3680 ± 318	13.9 ± 1.2
	K_{eff} (×10^3 M^{-1} s^{-1})	1386	700	56.3	24.2	0.038	2.8
AroE WT	k_{cat} (s^{-1})	307 ± 7	302 ± 7	2.9 ± 0.1	16.1 ± 1.6	NA	NA
	K_m (μM)	178 ± 14	55 ± 6	180 ± 13	7366 ± 961		
	K_{eff} (×10^3 M^{-1} s^{-1})	1724	5472	16.1	2.2		
Ael1 T15S	k_{cat} (s^{-1})	8.3 ± 0.2	8.8 ± 0.3	9.8 ± 0.1	22.2 ± 1.3	0.10 ± 0.01	0.015 ± 0.0003
	K_m (μM)	13.6 ± 1.6	16.9 ± 1.6	628 ± 21	2504 ± 266	5102 ± 883	13.8 ± 1.4
	K_{eff} (×10^3 M^{-1} s^{-1})	620	521	15.6	8.9	0.020	1.1
Ael1 K66N	k_{cat} (s^{-1})	0.0011 ± 0.00004	0.0011 ± 0.00004	ND	ND	ND	ND
	K_m (μM)	12.4 ± 1.9	13.9 ± 2.1				
	K_{eff} (×10^3 M^{-1} s^{-1})	0.089	0.079				
Ael1 F101T	k_{cat} (s^{-1})	2.34 ± 0.05	2.01 ± 0.05	39.5 ± 0.7	77.0 ± 2.2	0.064 ± 0.005	0.022 ± 0.0006
	K_m (μM)	7.8 ± 0.7	6.1 ± 0.6	891 ± 35	2338 ± 127	3278 ± 457	4.3 ± 0.8
	K_{eff} (×10^3 M^{-1} s^{-1})	300	330	44.3	32.9	0.020	5.1
Ael1 D102N	k_{cat} (s^{-1})	0.0004 ± 0.00002	0.0006 ± 0.000002	ND	ND	ND	ND
	K_m (μM)	24.3 ± 6.6	9.1 ± 1.6				
	K_{eff} (×10^3 M^{-1} s^{-1})	0.016	0.066				

[a]Kinetic parameters were determined at pH 8.8 and 25 °C by varying either the amount of substrate or the amount of cofactor while keeping the other at a fixed concentration of 2 mM. The reagent held at the fixed concentration is shown in parentheses. $K_{eff} = k_{cat}/K_m$. Abbreviations: WT, wild-type; SA, shikimate; QA, quinate; NA, no measurable activity; ND, not determined.

dx.doi.org/10.1021/bi200586y | *Biochemistry* 2011, 50, 8616−8627

Table 3. Kinetic Properties of YdiB Wild-Type Enzyme and Mutant Variants[a]

enzyme	parameter	SA(nad)	NAD(sa)	QA(nad)	NAD(qa)
YdiB WT	k_{cat} (s^{-1})	92.6 ± 2.8	77.7 ± 1.6	110 ± 3	105 ± 2
	K_m (μM)	4371 ± 229	311 ± 21	727 ± 52	485 ± 32
	K_{eff} ($\times 10^3$ M^{-1} s^{-1})	21.2	250	151	217
YdiB K74A	k_{cat} (s^{-1})	0.0003 ± 0.00002	0.0002 ± 0.00001	0.00007 ± 0.000003	0.0002 ± 0.000005
	K_m (μM)	3620 ± 788	231 ± 43	635 ± 78	674 ± 52
	K_{eff} ($\times 10^3$ M^{-1} s^{-1})	0.00008	0.0009	0.00001	0.0003
YdiB K74N	k_{cat} (s^{-1})	0.0169 ± 0.0012	0.0108 ± 0.0005	0.0172 ± 0.0004	0.0186 ± 0.0006
	K_m (μM)	4885 ± 716	987 ± 111	973 ± 57	698 ± 66
	K_{eff} ($\times 10^3$ M^{-1} s^{-1})	0.003	0.01	0.02	0.03
YdiB D110A	k_{cat} (s^{-1})	0.0020 ± 0.0002	0.0016 ± 0.00006	0.0026 ± 0.00008	0.0026 ± 0.00007
	K_m (μM)	3923 ± 758	254 ± 29	994 ± 76	457 ± 36
	K_{eff} ($\times 10^3$ M^{-1} s^{-1})	0.0005	0.006	0.003	0.006
YdiB D110N	k_{cat} (s^{-1})	0.012 ± 0.001	0.0080 ± 0.0002	0.0111 ± 0.0004	0.0238 ± 0.0007
	K_m (μM)	3294 ± 563	430 ± 29	955 ± 90	1114 ± 77
	K_{eff} ($\times 10^3$ M^{-1} s^{-1})	0.004	0.018	0.01	0.02

[a]Kinetic parameters were determined at pH 8.8 and 25 °C by varying either the amount of substrate or the amount of cofactor while keeping the other at a fixed concentration of 5 mM. The reagent held at the fixed concentration is shown in parentheses. $K_{eff} = k_{cat}/K_m$. Abbreviations: WT, wild-type; SA, shikimate; QA, quinate.

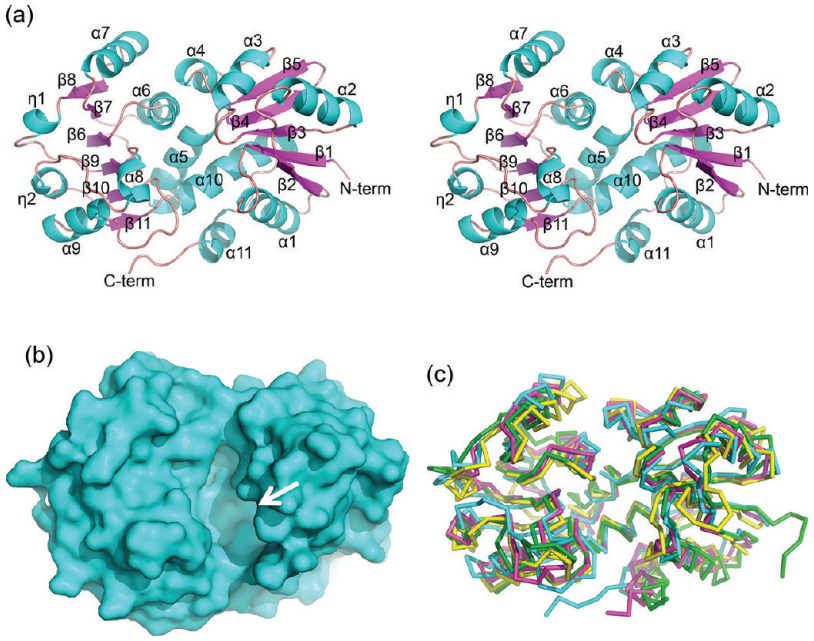

Figure 2. (a) Stereoview of the crystal structure of *P. putida* Ael1. Helices are colored blue, while β-strands are colored pink. The two α/β domains of the protein are connected centrally by α-helices α5 and α10. (b) Surface rendering of Ael1. The substrate and cofactor binding sites are found in the interdomain cleft marked with an arrow. (c) Main chain superimposition of representative structures of the members of the SDH family. The overall structures of *P. putida* Ael1 (blue), *T. thermophilus* AroE (pink; PDB entry 1WXD), *C. glutamicum* YdiB (yellow; PDB entry 2NLO), and *H. influenzae* SdhL (green; PDB entry 1NPY) are highly conserved.

α/β domains of the protein (Figure 2b). We were unable to obtain a liganded structure of Ael1 through cocrystallization studies. Therefore, we positioned $NADP^+$ and shikimate in the Ael1 structure by superimposition with the *T. thermophilus* AroE–shikimate–$NADP^+$ complex (PDB entry 2EV9) to identify residues that coordinate cofactor and substrate binding (Figure 3).[18] In the cofactor binding site, Ala128, Gly129, Gly130, and Ala131 form a glycine-rich loop responsible for anchoring the pyrophosphate moiety of NAD(P)$^+$ (Figure 3a). In $NADP^+$-binding enzymes, additional interactions with the cofactor are made by residues comprising the "basic patch" motif, NRTXXR/K. The penultimate arginine in this motif interacts with the adenine ribose phosphate of $NADP^+$ and is thus important for discriminating between $NADP^+$ and NAD^+.[14,18,22,25,37]

While we observe the arginine typical of $NADP^+$-binding enzymes in the Ael1 structure (Arg152), the Ael1 cofactor binding site also contains an aspartate (Asp153) that replaces the threonine in the $NADP^+$-binding motif (Figure 3a). The presence of this aspartate is somewhat surprising, as the negative charge of the residue is expected to repel the $NADP^+$ adenine ribose phosphate.[14] A corresponding aspartate had been observed in the cofactor binding sites of YdiB enzymes, which favor NAD^+.[14,23] However, unlike these enzymes, Ael1 preferentially utilizes $NADP^+$ (K_m = 12.0 ± 1.3 μM) instead of NAD^+ (K_m > 3 mM) (Table 2). Replacing $NADP^+$ with

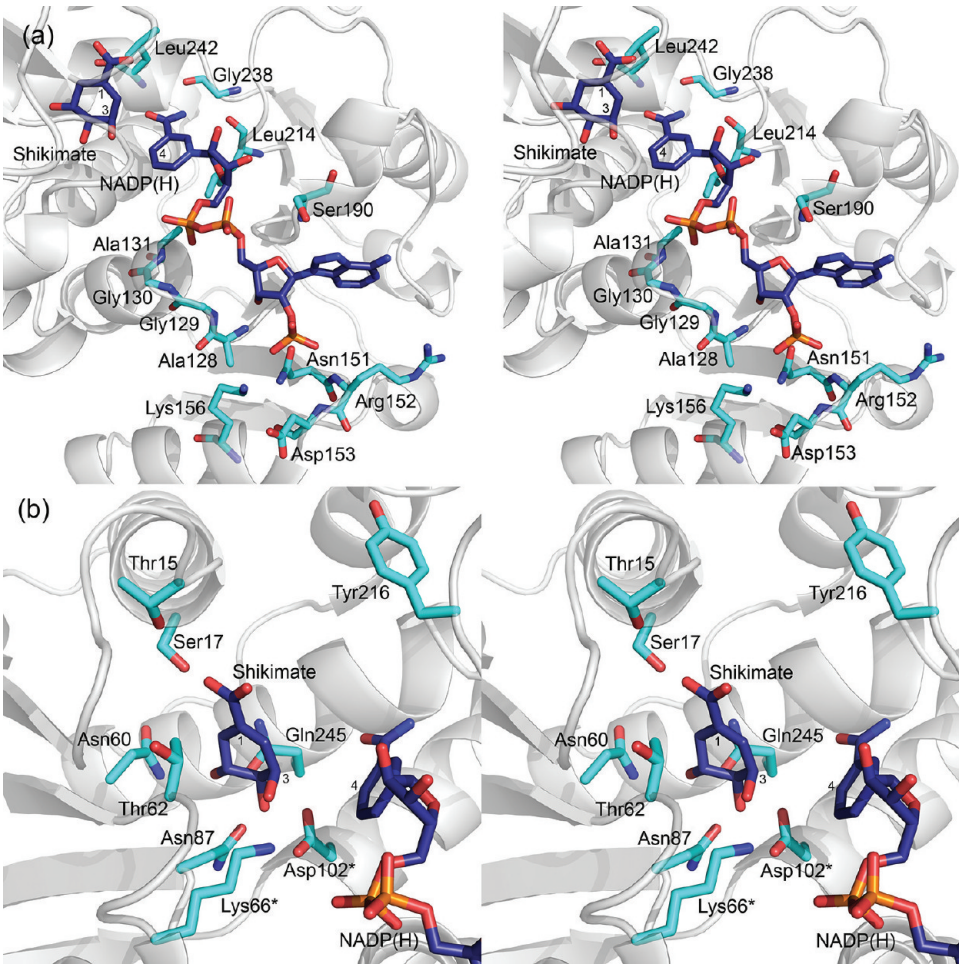

Figure 3. Stereoviews of key residues in the (a) cofactor and (b) substrate binding sites of *P. putida* Ael1. $NADP^+$ and shikimate are positioned by superimposition with the *T. thermophilus* AroE–shikimate–$NADP^+$ complex (PDB entry 2EV9). Residues predicted to be involved in cofactor or substrate recognition are shown as sticks. The putative catalytic residues are marked with asterisks.

NAD^+ results in a >100-fold increase in the *K*m of Ael1 for shikimate (Table 2). We hypothesize that to achieve efficient $NADP^+$ binding, Ael1 Asp153 adopts a conformation that minimizes electrostatic repulsion by the phosphate group of the cofactor. This conformation may be similar to that seen in our unliganded structure (Figure 3a).

Substrate Binding Site. A comparison of the structure of *P. putida* Ael1 and representative structures of AroE (Figure 4a) and YdiB (Figure 4b) reveals nearly complete conservation of substrate binding residues.[18] While Ael1 and the SdhL enzyme from *H. influenzae* share the majority of residues predicted to interact with the shikimate hydroxyl groups, SdhL displays more variability among residues that interact with the C1-carboxyl of the substrate (Figure 4c).[15] This distinction is likely indicative of an altered substrate preference for SdhL.

By analogy to the reported roles of the binding site residues of AroE,[18,24] Ael1 Thr15 and Ser17 are expected to bind the shikimate carboxyl. Thr15 replaces a highly conserved serine observed in all AroE structures and represents the only difference among the substrate binding groups of Ael1 and AroE (Figure 4a). Given the similar physiochemical properties of the two residues, Ael1 Thr15 likely retains the functional role of the AroE serine in substrate binding. Consistent with this hypothesis, mutation of Ael1 Thr15 to a serine resulted in a modest 2.4-fold increase in the K_m value for shikimate with $NADP^+$ as the cofactor (Table 2). An additional contact with the shikimate C1-carboxyl may be made by Ael1 Tyr216, a residue thought to function primarily in orienting the substrate in a position favorable for catalysis and in stabilizing the catalytic intermediate, rather than in an initial binding interaction.[21,24]

Further analysis of the Ael1 structure suggests that Thr62 may bind the shikimate C3-hydroxyl, while Asn87 and Gln245 are likely to bind the C4- and C5-hydroxyl groups of the substrate (Figure 4a). The latter residues are absolutely conserved among SDH homologues. The C5-hydroxyl of shikimate may also form a hydrogen bond with Asn60, an interaction that has been observed in some AroE–shikimate complexes.[18,21] A corresponding asparagine is absent from the *H. influenzae* SdhL structure, replaced with an alanine (Figure 4c), and from the structures of some AroE and YdiB enzymes.[14,15,24] These enzymes may instead utilize a glutamine corresponding to SdhL Gln246 to bind the shikimate C5-hydroxyl (Figure 4c).

In addition to shikimate, Ael1 is capable of catalyzing the oxidation of quinate, although its efficiency with the substrate is low compared to that of *P. putida* YdiB (Table 3). To explore the structural basis of quinate utilization by Ael1, we compared the structure of Ael1 and the quinate-liganded structure of the

dx.doi.org/10.1021/bi200586y | *Biochemistry* 2011, 50, 8616–8627

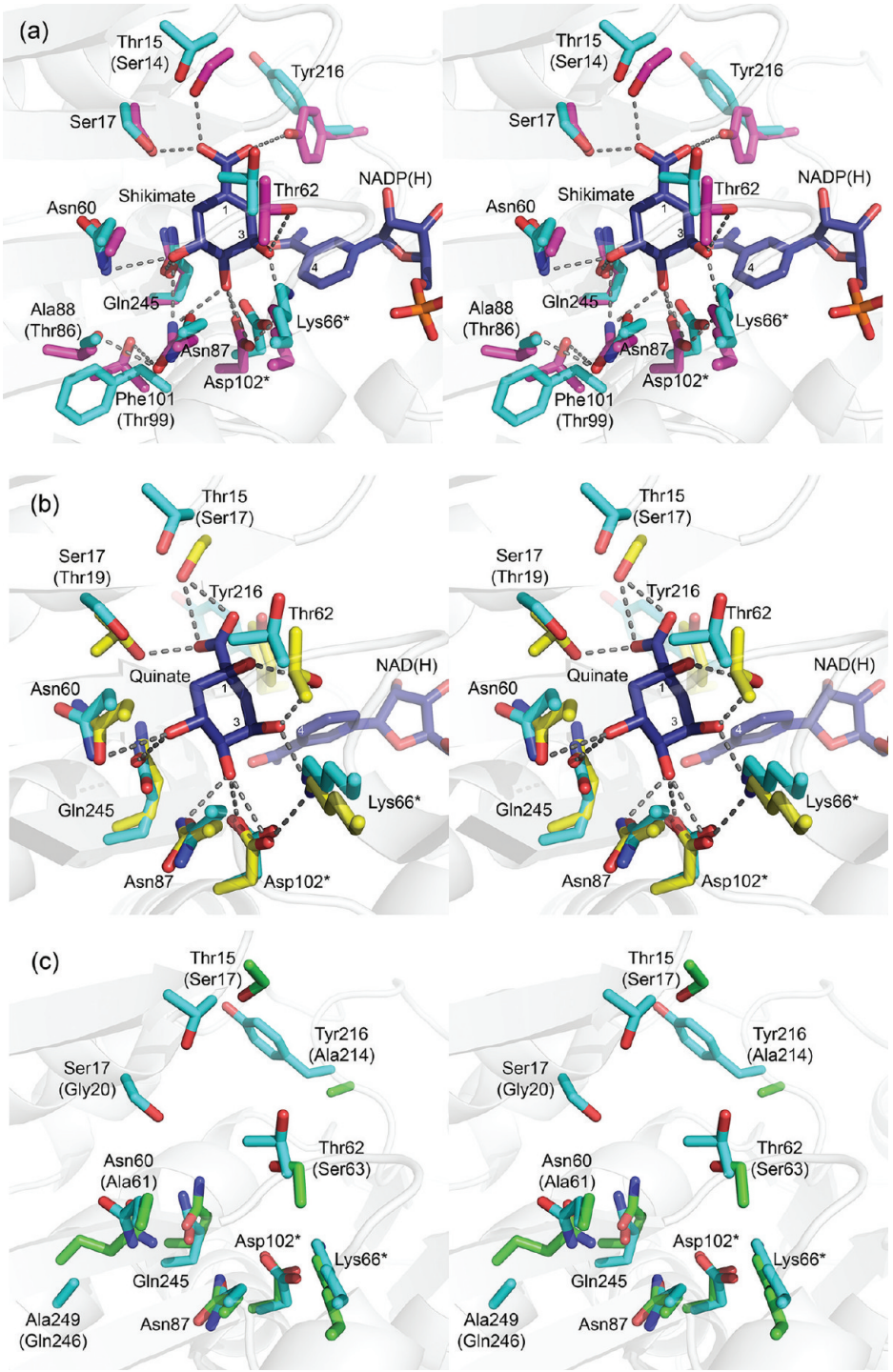

Figure 4. Comparison of the substrate binding sites of *P. putida* Ael1 and the other members of the SDH family. (a) Stereoview superimposition of the active sites of Ael1 (blue) and *T. thermophilus* AroE in complex with shikimate and NADP(H) (pink; PDB entry 2EV9). Residues that interact with the substrate are shown as sticks and numbered according to the Ael1 sequence. Where residue variations exist, the corresponding AroE residues are shown in parentheses. Potential interactions in the AroE−shikimate−$NADP^+$ complex are shown as dashed lines. The putative catalytic residues are marked with asterisks. Key substrate binding residues and a putative catalytic group, Asp102, are supported by polar residues in a secondary layer of the AroE active site. These polar groups are replaced with hydrophobic residues in the Ael1 structure. (b) Superimposition of the active sites of Ael1 (blue) and *C. glutamicum* YdiB in complex with quinate and NAD(H) (yellow; PDB entry 3JYP). Potential interactions in the YdiB−shikimate−NAD^+ complex are shown as dashed lines. (c) Superimposition of the active sites of Ael1 (blue) and *H. influenzae* SdhL (green; PDB entry 1NPY).

YdiB enzyme from *C. glutamicum* (PDB entry 3JYP). In the *C. glutamicum* YdiB−quinate−NAD(H) complex, Thr69 (corresponding to Ael1 Thr62) is positioned to coordinate the binding of the quinate C1-hydroxyl (Figure 4b). Because Ael1 also accepts quinate as a substrate, we propose that Ael1 Thr62 may participate in a similar interaction. Interestingly, AroE-type enzymes also possess a corresponding threonine (Figure 4a) yet are unable to utilize quinate as a substrate. It is

dx.doi.org/10.1021/bi200586y | *Biochemistry* 2011, 50, 8616–8627

therefore likely that subtle differences in the positioning of conserved active site residues are important for the varying affinity for quinate observed among the SDH homologues.

Contribution of Secondary Shell Residues to Substrate Binding and Catalysis. While residues predicted to directly interact with the substrate are highly conserved between the SDH subclasses, examination of a more distal, secondary "shell" of the Ael1 active site reveals a number of notable differences between Ael1 and previous SDH structures. Ael1 Phe101 replaces a threonine observed in other SDH structures (e.g., *T. thermophilus* AroE Thr99) (Figure 4a). This residue is responsible for positioning Asp102, a residue we predict to be catalytically important, and for orienting the substrate binding groups, Asn87 and Gln245.[24,38] Mutation of Ael1 Phe101 to threonine results in a 3.5-fold decrease in turnover rate (Table 2), an effect that may be attributable to the less than optimal positioning of the putative catalytic residue, Asp102, in the Phe101Thr variant. To accommodate the bulky side chain of Phe101, a second highly conserved threonine (*T. thermophilus* AroE Thr86) is substituted in the Ael1 structure with Ala88, replacing a potential hydrogen bonding network with hydrophobic interactions (Figure 4a). The proximity of these variations to key binding residues and the predicted catalytic groups is likely to contribute to the distinct kinetic properties of Ael1.

Putative Catalytic Residues. Comparison of the structures of Ael1, AroE, YdiB, and SdhL illustrates the conserved placement of a pair of ionizable active site residues (Figure 4).[14,15,24] These residues, corresponding to Ael1 Lys66 and Asp102, represent the most likely candidates for participating in the catalytic mechanism of the enzymes. Catalysis in the SDH family has been proposed to proceed via a general acid−base mechanism in which the invariant lysine and aspartate function as a catalytic dyad.[15,20,24] The structures of AroE and YdiB in complex with shikimate (or quinate) and NAD(P)(H) demonstrate the proximity of the purported catalytic residues and the reactive C3-hydroxyl of the substrate (Figure 4a,b).[18,20,24] Moreover, the structures place the C4-nicotinamide of the cofactor in the vicinity of the bound substrate to coordinate a hydride transfer from C3 of the substrate.

Surprisingly, the conserved active site lysine and aspartate have been reported to function in substrate binding rather than catalysis in a YdiB enzyme from *E. coli*, suggesting that some members of the SDH family use a catalytic mechanism that differs from the proposed acid−base reaction.[26] We were therefore interested in exploring the catalytic mechanism utilized by Ael1, an enzyme for which no mechanistic data previously existed. We mutated the Ael1 active site lysine and aspartate and examined the effect on catalysis by steady state kinetic analysis. Ael1 Lys66 and Asp102 were independently replaced with asparagine to minimize changes in side chain van der Waals volumes. These substitutions directly address the mechanistic role of the ionizable residues by eliminating their charge effect and, consequently, their ability to participate in the catalyzed reaction. Analysis by size exclusion chromatography demonstrated that the Ael1 wild-type and variant proteins are eluted with a similar profile and retention time, indicating that the mutations do not cause global structural perturbations or aberrant protein aggregation.

Both the Lys66Asn and Asp102Asn mutants exhibited a dramatic reduction in turnover rate (Table 2). The Lys66Asn variant displayed a 7000-fold decrease in k_{cat} using shikimate and $NADP^+$ compared to that of the wild-type enzyme. Mutating Asp102 resulted in a 20000-fold reduction in k_{cat}. The active site mutations had a relatively small impact on the Michaelis constant, with *K*m values for shikimate between 2 and 4 times that of the wild-type enzyme (Table 2). These mutations clearly demonstrate the essential nature of the conserved lysine and aspartate in the activity of Ael1.

Catalytic Mechanism of *P. putida* YdiB. *P. putida* also encodes an NAD^+-dependent quinate/shikimate dehydrogenase belonging to the YdiB subclass.[13] Given the possibility that YdiB enzymes may use a distinct catalytic mechanism, we investigated the mechanism employed by the *P. putida* enzyme. We generated both asparagine and alanine mutants of the active site Lys74 and Asp110 and measured their activity in the presence of shikimate or quinate and NAD^+ (Table 3). The wild-type and mutant proteins all had similar elution profiles when subjected to size exclusion chromatography.

The Lys74Asn mutant exhibited a 5000-fold decrease in k_{cat} compared to that of the wild-type enzyme using shikimate as its substrate and a 6000-fold decrease using quinate. Similarly, the Asp110Asn mutant displayed 7000- and 10000-fold reductions in k_{cat} using shikimate and quinate, respectively. Both mutants showed relatively minor changes in K_m with either substrate (Table 3). The effects of the Lys74Ala and Asp110Ala mutations were even more pronounced, likely because of the smaller van der Waals volume occupied by alanine compared to the wild-type residues. These mutations resulted in decreases in k_{cat} in excess of 40000-fold but still caused only small alterations in K_m (Table 3).

Substrate Binding Analysis. We have shown by kinetic analysis that mutation of the active site lysine or aspartate of *P. putida* Ael1 and YdiB results in a dramatic reduction in the catalytic activity of the enzymes with little effect on their K_m values. To further evaluate the impact of the mutations on substrate binding, we attempted isothermal titration calorimetry; however, the binding of substrate did not produce a measurable change in enthalpy. We therefore used differential static light scattering (DSLS) for our analysis of substrate binding. DSLS is a technique that monitors temperature-dependent protein aggregation.[28,39] The binding of a ligand increases the thermostability of a protein in a concentration-dependent manner.[28,40,41] This effect can be quantified as a change in the temperature of aggregation of the protein bound to the ligand relative to the apoprotein and can be expressed as ΔT_{agg}.

We observed a clear concentration-dependent increase in the thermostability of the YdiB wild-type enzyme in the presence of quinate, the preferred substrate of the enzyme (Figure 5a). By plotting ΔT_{agg} as a function of quinate concentration, we generated a substrate binding profile for the wild-type enzyme (Figure 5b). We found that the YdiB K74N and D110A variants were similarly stabilized by quinate in a concentration-dependent manner. In fact, these mutants yielded binding profiles that were virtually identical to that of the wild-type protein, demonstrating that their affinity for the substrate is not reduced compared to that of the wild-type enzyme (Figure 5b). When taken together with our kinetic analysis, our data therefore suggest that the YdiB active site lysine and aspartate are not essential for substrate binding but instead are key catalytic residues.

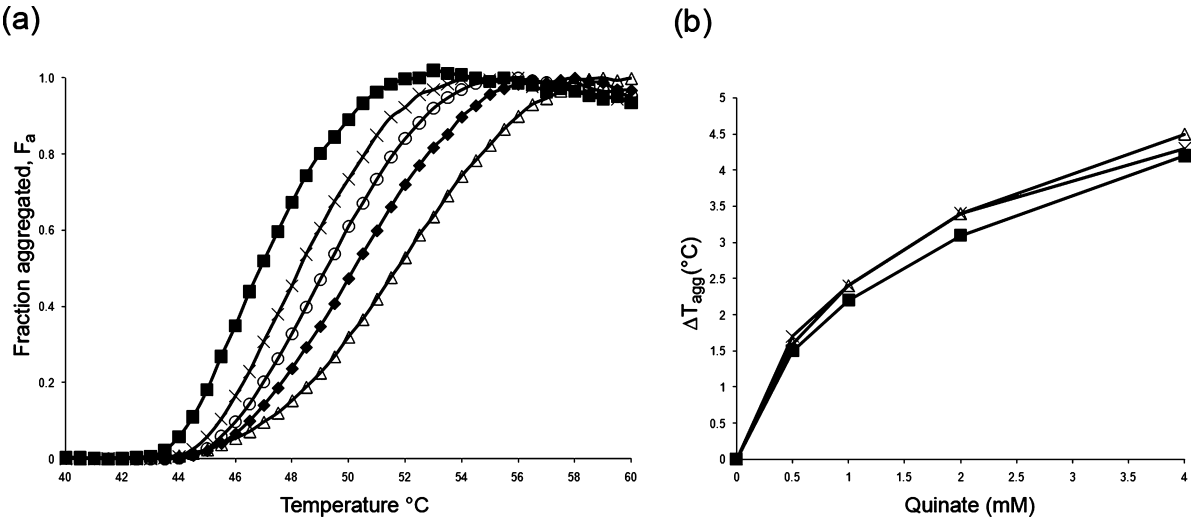

Figure 5. DSLS analysis of quinate binding by the YdiB wild-type enzyme and K74A and D110N mutants. (a) Representative plot showing the dependency of the thermostability of wild-type YdiB on quinate concentration: 0 (■), 0.5 (×), 1 (○), 2 (◆), and 4 mM (△). (b) Change in thermostability, ΔT_{agg}, of YdiB wild-type (■), K74A (△), and D110N (×) enzymes as a function of quinate concentration.

■ DISCUSSION

The conservation of the shikimate pathway in pathogenic bacteria and fungi as well as apicomplexan parasites and weed plants implies that inhibitors of the pathway could have valuable medical and agricultural applications. Indeed, the most effective inhibitor of the shikimate pathway identified to date, glyphosate, has been used extensively as a herbicide and has been shown to limit the growth of the malarial parasite *Plasmodium falciparum*.[3] Recently, a number of weed plants have evolved glyphosate resistance, renewing the urgency to develop novel inhibitors of the shikimate pathway.[8,9] Given its central role in the pathway, AroE is an appealing target for these inhibitors. However, the in vivo efficacy of drugs acting against AroE could be affected by the existence of additional SDH homologues, such as Ael1, that may be capable of functionally compensating for the inhibited enzyme. Evidence of structural and mechanistic conservation within the SDH family may therefore be useful in designing drugs capable of broadly inhibiting the different members of the family.

To this end, we have determined the first representative crystal structure of an Ael1 enzyme (Figure 2a). No structural data were available for the Ael1 subclass prior to this study. The overall structure of Ael1 is very similar to those of other SDH homologues, demonstrating strong conservation of the three-dimensional fold in the SDH family (Figure 2c). We also observe nearly complete conservation of residues predicted to interact with the substrate shikimate (or quinate) in the Ael1, AroE, and YdiB subclasses and significant conservation in the SdhL subclass (Figure 4).

Although *P. putida* Ael1 shares all but a single substrate binding residue with AroE (Figure 4a), the enzyme nevertheless possesses a distinct kinetic profile (Table 2). In particular, it displays a 31-fold lower Michaelis constant with respect to shikimate and a 39-fold lower catalytic constant compared to the AroE enzyme from the same organism (Table 2). We identified variations in a distal layer of the Ael1 active site that may contribute to these kinetic properties (Figure 4a). These secondary shell residues appear to play important roles in positioning key binding and catalytic groups. However, mutation of these residues and kinetic analysis suggest that differences in residue composition alone are insufficient to explain the distinct kinetic properties of Ael1 (Table 2). It is therefore likely that main chain dynamics make a significant contribution to the activity of the enzyme.

Further comparison of the structure of Ael1 with other SDH structures identifies the invariant active site lysine and aspartate (Figure 4), residues that have been proposed to participate in catalysis in the AroE and SdhL subclasses via a general acid–base mechanism.[20] While these residues are strictly conserved in the SDH family, their mechanistic role among different SDH homologues is still debated. Here, we have established through site-directed mutagenesis that the two residues are functioning as a catalytic dyad in *P. putida* Ael1. That is, mutation of either residue results in a large decrease in turnover rate with only minor changes in the Michaelis constant (Table 2). A previous study has demonstrated that mutation of the corresponding active site lysine or aspartate in *Arabidopsis* AroE similarly causes a significant reduction in k_{cat}, with only limited effects on K_m.[24] Additional work has shown that mutation of either residue in the SdhL enzyme from *H. influenzae* inactivates the enzyme, further demonstrating the critical role of these groups in catalysis.[15] Taken together, these results suggest that Ael1, AroE, and SdhL employ an equivalent catalytic mechanism requiring the active site lysine and aspartate.

This mechanism is controversial for the YdiB subclass, as the lysine and aspartate have been reported to function in substrate binding instead of catalysis in a YdiB enzyme from *E. coli*.[26] The potential for conserved residues to have distinct biochemical roles in different SDH homologues could confound attempts to rationally target the active sites of the enzymes for drug design. It is possible that shikimate and quinate are bound in the active site of *E. coli* YdiB in an orientation that differs from that observed in previous liganded SDH structures. Repositioning of the substrate may alter the functional roles of active site residues. However, the *C. glutamicum* YdiB–shikimate–NAD(H) and YdiB–quinate–NAD(H) complexes reveal that the substrates are bound in the expected orientation in at least some YdiB enzymes, with their reactive C3-hydroxyl groups positioned adjacent to the active site lysine and aspartate (Figure 4b).[24] This

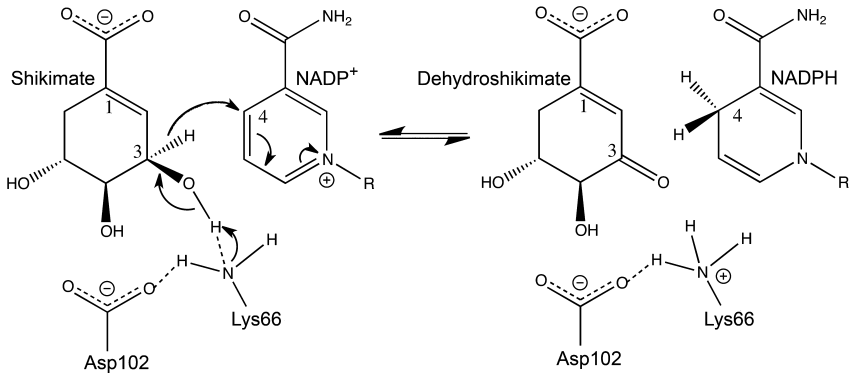

Figure 6. Proposed reaction mechanism for the members of the SDH family.

observation supports the role of these residues in catalysis for some members of the YdiB subclass.

We used site-directed mutagenesis to investigate the catalytic mechanism employed by a representative of the YdiB subclass from *P. putida*, an enzyme with a sequence that is 51 and 29% identical with those of the YdiB enzymes from *C. glutamicum* and *E. coli*, respectively (25% identical with that of *P. putida* Ael1). Sequence alignment reveals extensive conservation of key active site residues among the YdiB enzymes and the other subclasses in the SDH family (Figure 1). Mutation of the invariant lysine or aspartate of *P. putida* YdiB resulted in a pronounced reduction in turnover rate (Table 3). To determine whether the reduced activity is the result of decreased catalytic capacity or an inability of the mutant enzymes to bind their substrates, we utilized DSLS. The results of this experiment demonstrated that the YdiB mutants bind quinate, the preferred substrate, with an affinity similar to that of the wild-type enzyme, indicating that substrate binding is not compromised. Thus, the dramatic reduction in enzymatic activity seen in the mutant variants is attributed to the fact that both Lys74 and Asp110 are important catalytic residues in *P. putida* YdiB. This result is in contrast to the reported function of the residues in *E. coli* YdiB.[26] Mutagenesis and kinetic analyses have therefore established a mechanistic role for these residues in catalysis for the Ael1, AroE, and SdhL subclasses as well as at least one member of the YdiB subclass. *E. coli* YdiB represents an interesting outlier among the members of the SDH family. Further structural and biochemical analysis of the enzyme will be important in understanding the basis of its distinct mechanistic attributes.

On the basis of our findings, we speculate that the reaction mechanism for the members of the SDH family is similar to that suggested by Gan et al.[20] The reaction is shown in Figure 6. Briefly, a hydride transferred to the C4-nicotinamide of $NAD(P)^+$ is coordinated with the removal of a proton from the C3-hydroxyl group of shikimate or quinate by the invariant active site lysine. The lysine is stabilized by the nearby aspartate, which may facilitate the transfer of a proton from the ionized lysine to the bulk solvent via a conserved water molecule.[20] The use of an acid−base dyad in reaction mechanisms is not uncommon and has been observed in other enzyme systems, such as dTDP-6-deoxy-D-xylo-4-hexulose 3,5-epimerase (RmlC) and members of the enolase family, including mandelate racemase.[42−44] The results presented here argue for a conserved catalytic mechanism in the SDH family, a feature that will facilitate the design of inhibitors targeting the enzymes.

■ ASSOCIATED CONTENT

Accession Codes

The atomic coordinates and structure factors for Ael1 have been deposited in the Protein Data Bank, Research Collaboratory for Structural Bioinformatics, Rutgers University, New Brunswick, NJ as entry 3PWZ.

■ AUTHOR INFORMATION

Corresponding Author

*Address: 25 Willcocks St., Toronto, Ontario, Canada M5S 3B2. Telephone: (416) 946-8337. Fax: (416) 978-5878. E-mail: dinesh.christendat@utoronto.ca.

Funding

This work was supported with funds from a Natural Sciences and Engineering Research Council of Canada (NSERC) discovery grant to D.C. J.P. is supported by an NSERC postgraduate scholarship.

■ ACKNOWLEDGMENTS

We acknowledge the Centre for the Analysis of Genome Evolution & Function for sequencing support and the Structural Genomics Consortium Toronto for use of their Stargazer ligand screening platform. We thank Masoud Vedadi for providing technical guidance in conducting the ligand binding study. X-ray crystallographic results shown in this report are derived from work performed at Argonne National Laboratory, Structural Biology Center at the Advanced Photon Source. Argonne is operated by UChicago Argonne, LLC, for the U.S. Department of Energy, Office of Biological and Environmental Research under Contract DE-AC02-06CH11357. X-ray crystallographic data were collected at beamline 19-ID.

■ ABBREVIATIONS

SDH, shikimate dehydrogenase; EPSP synthase, enolpyruvyl-shikimate-3-phosphate synthase; SdhL, shikimate dehydrogenase-like; Ael1, AroE-like1; DSLS, differential static light scattering; rmsd, root-mean-square deviation; RmlC, dTDP-6-deoxy-D-xylo-4-hexulose 3,5-epimerase.

■ REFERENCES

(1) Herrmann, K. M. (1995) The Shikimate Pathway: Early Steps in the Biosynthesis of Aromatic Compounds. *Plant Cell 7*, 907−919.

(2) Herrmann, K. M., and Weaver, L. M. (1999) The Shikimate Pathway. *Annu. Rev. Plant Physiol. Plant Mol. Biol. 50*, 473−503.

(3) Roberts, F., Roberts, C. W., Johnson, J. J., Kyle, D. E., Krell, T., Coggins, J. R., Coombs, G. H., Milhous, W. K., Tzipori, S., Ferguson,

D. J., Chakrabarti, D., and McLeod, R. (1998) Evidence for the shikimate pathway in apicomplexan parasites. *Nature 393*, 801−805.

(4) Han, C., Wang, L., Yu, K., Chen, L., Hu, L., Chen, K., Jiang, H., and Shen, X. (2006) Biochemical characterization and inhibitor discovery of shikimate dehydrogenase from Helicobacter pylori. *FEBS J. 273*, 4682−4692.

(5) Coggins, J.R., Abell, C., Evans, L. B., Frederickson, M., Robinson, D. A., Roszak, A. W., and Lapthorn, A. P. (2003) Experiences with the shikimate-pathway enzymes as targets for rational drug design. *Biochem. Soc. Trans. 31*, 548−552.

(6) Schonbrunn, E., Eschenburg, S., Shuttleworth, W. A., Schloss, J. V., Amrhein, N., Evans, J. N., and Kabsch, W. (2001) Interaction of the herbicide glyphosate with its target enzyme 5-enolpyruvylshikimate 3-phosphate synthase in atomic detail. *Proc. Natl. Acad. Sci. U.S.A. 98*, 1376−1380.

(7) Steinrücken, H. C., and Amrhein, N. (1980) The herbicide glyphosate is a potent inhibitor of 5-enolpyruvyl-shikimic acid-3-phosphate synthase. *Biochem. Biophys. Res. Commun. 94*, 1207−1212.

(8) Powles, S. B. (2008) Evolved glyphosate-resistant weeds around the world: Lessons to be learnt. *Pest Manage. Sci. 64*, 360−365.

(9) Vila-Aiub, M. M., Vidal, R. A., Balbi, M. C., Gundel, P. E., Trucco, F., and Ghersa, C. M. (2008) Glyphosate-resistant weeds of South American cropping systems: An overview. *Pest Manage. Sci. 64*, 366−371.

(10) Pittard, J., and Wallace, B. J. (1966) Gene controlling the uptake of shikimic acid by *Escherichia coli*. *J. Bacteriol. 92*, 1070−1075.

(11) Pittard, J., and Wallace, B. J. (1966) Distribution and function of genes concerned with aromatic biosynthesis in *Escherichia coli*. *J. Bacteriol. 91*, 1494−1508.

(12) Fonseca, I. O., Magalhaes, M. L., Oliveira, J. S., Silva, R. G., Mendes, M. A., Palma, M. S., Santos, D. S., and Basso, L. A. (2006) Functional shikimate dehydrogenase from *Mycobacterium tuberculosis* H37Rv: Purification and characterization. *Protein Expression Purif. 46*, 429−437.

(13) Singh, S., Stavrinides, J., Christendat, D., and Guttman, D. S. (2008) A phylogenomic analysis of the shikimate dehydrogenases reveals broadscale functional diversification and identifies one functionally distinct subclass. *Mol. Biol. Evol. 25*, 2221−2232.

(14) Michel, G., Roszak, A. W., Sauve, V., Maclean, J., Matte, A., Coggins, J. R., Cygler, M., and Lapthorn, A. J. (2003) Structures of shikimate dehydrogenase AroE and its Paralog YdiB. A common structural framework for different activities. *J. Biol. Chem. 278*, 19463−19472.

(15) Singh, S., Korolev, S., Koroleva, O., Zarembinski, T., Collart, F., Joachimiak, A., and Christendat, D. (2005) Crystal structure of a novel shikimate dehydrogenase from *Haemophilus influenzae*. *J. Biol. Chem. 280*, 17101−17108.

(16) Giles, N. H., Case, M. E., Baum, J., Geever, R., Huiet, L., Patel, V., and Tyler, B. (1985) Gene organization and regulation in the qa (quinic acid) gene cluster of *Neurospora crassa*. *Microbiol. Rev. 49*, 338−358.

(17) Knop, D. R., Draths, K. M., Chandran, S. S., Barker, J. L., von Daeniken, R., Weber, W., and Frost, J. W. (2001) Hydroaromatic equilibration during biosynthesis of shikimic acid. *J. Am. Chem. Soc. 123*, 10173−10182.

(18) Bagautdinov, B., and Kunishima, N. (2007) Crystal structures of shikimate dehydrogenase AroE from *Thermus thermophilus* HB8 and its cofactor and substrate complexes: Insights into the enzymatic mechanism. *J. Mol. Biol. 373*, 424−438.

(19) Benach, J., Lee, I., Edstrom, W., Kuzin, A. P., Chiang, Y., Acton, T. B., Montelione, G. T., and Hunt, J. F. (2003) The 2.3-Å crystal structure of the shikimate 5-dehydrogenase orthologue YdiB from *Escherichia coli* suggests a novel catalytic environment for an NAD-dependent dehydrogenase. *J. Biol. Chem. 278*, 19176−19182.

(20) Gan, J., Wu, Y., Prabakaran, P., Gu, Y., Li, Y., Andrykovitch, M., Liu, H., Gong, Y., Yan, H., and Ji, X. (2007) Structural and biochemical analyses of shikimate dehydrogenase AroE from *Aquifex aeolicus*: Implications for the catalytic mechanism. *Biochemistry 46*, 9513−9522.

(21) Han, C., Hu, T., Wu, D., Qu, S., Zhou, J., Ding, J., Shen, X., Qu, D., and Jiang, H. (2009) X-ray crystallographic and enzymatic analyses of shikimate dehydrogenase from *Staphylococcus epidermidis*. *FEBS J. 276*, 1125−1139.

(22) Padyana, A.K., and Burley, S. K. (2003) Crystal structure of shikimate 5-dehydrogenase (SDH) bound to NADP: Insights into function and evolution. *Structure 11*, 1005−1013.

(23) Schoepe, J., Niefind, K., and Schomburg, D. (2008) 1.6 angstroms structure of an NAD^+-dependent quinate dehydrogenase from *Corynebacterium glutamicum*. *Acta Crystallogr. D64*, 803−809.

(24) Singh, S. A., and Christendat, D. (2006) Structure of *Arabidopsis* dehydroquinate dehydratase-shikimate dehydrogenase and implications for metabolic channeling in the shikimate pathway. *Biochemistry 45*, 7787−7796.

(25) Ye, S., Von Delft, F., Broun, A., Knuth, M. W., Swanson, R. V., and McRee, D. E. (2003) The crystal structure of shikimate dehydrogenase (AroE) reveals a unique NADPH binding mode. *J. Bacteriol. 185*, 4144−4151.

(26) Lindner, H. A., Nadeau, G., Matte, A., Michel, G., Menard, R., and Cygler, M. (2005) Site-directed mutagenesis of the active site region in the quinate/shikimate 5-dehydrogenase YdiB of *Escherichia coli*. *J. Biol. Chem. 280*, 7162−7169.

(27) Cleland, W.W. (1979) Statistical analysis of enzyme kinetic data. *Methods Enzymol. 63*, 103−138.

(28) Senisterra, G. A., Markin, E., Yamazaki, K., Hui, R., Vedadi, M., and Awrey, D. E. (2006) Screening for ligands using a generic and high-throughput light-scattering-based assay. *J. Biomol. Screening 11*, 940−948.

(29) Otwinowski, Z., and Minor, W. (1997) Processing of X-ray Diffraction Data Collected in Oscillation Mode. *Methods Enzymol. 276*, 307−326.

(30) Potterton, L., McNicholas, S., Krissinel, E., Gruber, J., Cowtan, K., Emsley, P., Murshudov, G. N., Cohen, S., Perrakis, A., and Noble, M. (2004) Developments in the CCP4 molecular-graphics project. *Acta Crystallogr. D60*, 2288−2294.

(31) Navaza, J. (2001) Implementation of molecular replacement in AMoRe. *Acta Crystallogr. D57*, 1367−1372.

(32) Emsley, P., and Cowtan, K. (2004) Coot: Model-building tools for molecular graphics. *Acta Crystallogr. D60*, 2126−2132.

(33) Murshudov, G. N., Vagin, A. A., and Dodson, E. J. (1997) Refinement of macromolecular structures by the maximum-likelihood method. *Acta Crystallogr. D53*, 240−255.

(34) Adams, P. D., Afonine, P. V., Bunkoczi, G., Chen, V. B., Davis, I. W., Echols, N., Headd, J. J., Hung, L. W., Kapral, G. J., Grosse-Kunstleve, R. W., McCoy, A. J., Moriarty, N. W., Oeffner, R., Read, R. J., Richardson, D. C., Richardson, J. S., Terwilliger, T. C., and Zwart, P. H. (2010) PHENIX: A comprehensive Python-based system for macromolecular structure solution. *Acta Crystallogr. D66*, 213−221.

(35) Lim, S., Schroder, I., and Monbouquette, H. G. (2004) A thermostable shikimate 5-dehydrogenase from the archaeon *Archaeoglobus fulgidus*. *FEMS Microbiol. Lett. 238*, 101−106.

(36) Zhang, X., Zhang, S., Hao, F., Lai, X., Yu, H., Huang, Y., and Wang, H. (2005) Expression, purification and properties of shikimate dehydrogenase from *Mycobacterium tuberculosis*. *J. Biochem. Mol. Biol. 38*, 624−631.

(37) Scrutton, N. S., Berry, A., and Perham, R. N. (1990) Redesign of the coenzyme specificity of a dehydrogenase by protein engineering. *Nature 343*, 38−43.

(38) Singh, S. A., and Christendat, D. (2007) The DHQ-dehydroshikimate-SDH-shikimate-NADP(H) Complex: Insights into Metabolite Transfer in the Shikimate Pathway. *Cryst. Growth Des. 7*, 2153−2160.

(39) Buchner, J., Schmidt, M., Fuchs, M., Jaenicke, R., Rudolph, R., Schmid, F. X., and Kiefhaber, T. (1991) GroE facilitates refolding of citrate synthase by suppressing aggregation. *Biochemistry 30*, 1586–1591.

(40) Vedadi, M., Arrowsmith, C. H., Allali-Hassani, A., Senisterra, G., and Wasney, G. A. (2010) Biophysical characterization of recombinant proteins: A key to higher structural genomics success. *J. Struct. Biol. 172*, 107–119.

(41) Vedadi, M., Niesen, F. H., Allali-Hassani, A., Fedorov, O. Y., Finerty, P. J. Jr., Wasney, G. A., Yeung, R., Arrowsmith, C., Ball, L. J., Berglund, H., Hui, R., Marsden, B. D., Nordlund, P., Sundstrom, M., Weigelt, J., and Edwards, A. M. (2006) Chemical screening methods to identify ligands that promote protein stability, protein crystallization, and structure determination. *Proc. Natl. Acad. Sci. U.S.A. 103*, 15835–15840.

(42) Babbitt, P. C., Hasson, M. S., Wedekind, J. E., Palmer, D. R., Barrett, W. C., Reed, G. H., Rayment, I., Ringe, D., Kenyon, G. L., and Gerlt, J. A. (1996) The enolase superfamily: A general strategy for enzyme-catalyzed abstraction of the α-protons of carboxylic acids. *Biochemistry 35*, 16489–16501.

(43) Christendat, D., Saridakis, V., Dharamsi, A., Bochkarev, A., Pai, E. F., Arrowsmith, C. H., and Edwards, A. M. (2000) Crystal structure of dTDP-4-keto-6-deoxy-D-hexulose 3,5-epimerase from *Methanobacterium thermoautotrophicum* complexed with dTDP. *J. Biol. Chem. 275*, 24608–24612.

(44) Dong, C., Major, L. L., Allen, A., Blankenfeldt, W., Maskell, D., and Naismith, J. H. (2003) High-resolution structures of RmlC from *Streptococcus suis* in complex with substrate analogs locate the active site of this class of enzyme. *Structure 11*, 715–723.